

Investigating the ultimate accuracy of Doppler-broadening thermometry by means of a global fitting procedure

Pasquale Amodio,¹ Maria Domenica De Vizia,¹ Luigi Moretti,^{1,*} and Livio Gianfrani^{1,2}

¹*Department of Mathematics and Physics, Second University of Naples, Viale Lincoln 5, 81100 Caserta, Italy*

²*INRIM-Istituto Nazionale di Ricerca Metrologica, Strada delle Cacce 91, 10135 Torino, Italy*

(Received 10 June 2015; published 8 September 2015)

Doppler-limited, high-precision, molecular spectroscopy in the linear regime of interaction may refine our knowledge of the Boltzmann constant. To this end, the global uncertainty in the retrieval of the Doppler width should be reduced down to 1 part over 10^6 , which is a rather challenging target. So far, Doppler-broadening thermometry has been mostly limited by the uncertainty associated to the line shape model that is adopted for the nonlinear least-squares fits of experimental spectra. In this paper, we deeply investigate this issue by using a very realistic and sophisticated model, known as partially correlated speed-dependent Keilson-Storer profile, to reproduce near-infrared water spectra. A global approach has been developed to fit a large number of numerically simulated spectra, testing a variety of simplified line-shape models. It turns out that the most appropriate model is the speed-dependent hard-collision profile. We demonstrate that the Doppler width can be determined with relative precision and accuracy, respectively, of 0.42 and 0.75 part per million.

DOI: [10.1103/PhysRevA.92.032506](https://doi.org/10.1103/PhysRevA.92.032506)

PACS number(s): 33.70.Jg, 33.20.Ea, 06.20.Jr, 42.62.Fi

I. INTRODUCTION

Doppler-broadening thermometry (DBT) is a relatively new approach of primary gas thermometry, which consists in retrieving the Doppler width ($\Delta\nu_D$) from the highly accurate observation of the profile of a given atomic or molecular line in a gas sample at the thermodynamic equilibrium [1,2]. If implemented at the temperature of the triple point of water (namely, $T = 273.16$ K), pursuing the highest levels of precision and accuracy for laser absorption spectroscopy in the linear regime of interaction, DBT can provide an optical determination of the Boltzmann constant (k_B), by inverting the following equation:

$$\Delta\nu_D = \frac{\nu_0}{c} \sqrt{2 \ln 2 \frac{k_B T}{M}}, \quad (1)$$

where ν_0 is the line center frequency, c is the speed of light, and M is the molecular mass. Therefore, DBT allows one to link the thermodynamic temperature to an absolute frequency (ν_0) and a frequency interval ($\Delta\nu_D$). In its best implementation, DBT has measured k_B with a global uncertainty of 24 parts over 10^6 by extrapolating the Doppler width from the shape of a H_2^{18}O transition at $1.4 \mu\text{m}$ [3]. In order to contribute to the new definition of unit kelvin, but also for being recognized as a useful tool for the realization of the future international temperature scale, DBT has to approach the target accuracy of 1 part per million (ppm) [4]. The Voigt function is the most used line profile in molecular spectroscopy. It derives from a simplified description of the collisional processes among the molecules, taking into account only those collisions that provide a dephasing of the molecular dipole and assuming that the collisional parameters are independent of the absorber velocity. Recent experiments have shown that the Voigt model is not sufficient to describe the physical situation of self-colliding molecules (namely, collisions between molecules of the same species), even in the Doppler regime [5,6]. The

net effect due to the velocity-changing collisions and speed dependence of collisional parameters is a line narrowing that should be considered by adopting sophisticated line shape models involving some characteristic parameters, whose values are not known with the necessary accuracy. Lemarchand *et al.*, in their mid-infrared implementation of DBT on ammonia, proposed to determine the collisional parameters for the selected line by doing spectral recordings at relatively high pressures (from 2 up to 25 Pa) in a single-pass isothermal cell [7]; then, the Boltzmann constant is determined from absorption spectra in a multipass cell at low pressures (variable between 0.1 and 2.5 Pa), taking advantage from the knowledge of the narrowing parameters. In their strategy, the Doppler width is fixed at the expected value when analyzing the high-pressure spectra, while it is a variable quantity in the fits of experimental low-pressure profiles. So doing, the French group has demonstrated that the relative uncertainty on k_B associated to the line-shape model can be as small as 1.8 ppm [7]. In this paper, we propose a radically different approach based upon the use of a global fitting procedure, which allows one to fit a number of spectra across a given pressure range, sharing some free parameters such as the Doppler width, the velocity-changing collision parameter, and the quantities m and n entering into the speed dependence of collisional broadening and shifting, respectively. The procedure was applied to a large number of numerically simulated spectra, as generated by using the partially correlated speed-dependent Keilson-Storer model. Recent studies have demonstrated that this latter is a very realistic model to describe H_2O line profiles in the near-infrared region [8,9]. In such a model, velocity changes are modeled by using the Keilson-Storer collision kernel with two characteristic parameters, which were deduced in Ref. [8] from classical molecular dynamics simulations. Comparisons between simulated spectra and measurements for several lines in the near-infrared at various pressures showed excellent agreements, thus demonstrating the validity of the model [8,9]. Unfortunately, due to its complexity and large computational cost, the profiles with Keilson-Storer collision kernel model cannot be implemented into a fitting routine. In

*luigi.moretti@unina2.it

this article, a variety of semiclassical models, characterized by a simplified collision kernel, were selected and tested with the aim of understanding which of them is capable of providing the best precision and accuracy in Doppler width retrievals. It turns out that the best performance is obtained by the speed-dependent hard-collision profile, which can lead to a sub-ppm precision and accuracy in the retrieval of the Doppler width. Therefore, our study demonstrates that the knowledge of collisional parameters is not an indispensable prerequisite for low-uncertainty DBT, provided that a global fitting approach is adopted. This makes DBT measurements more robust, reliable, self-consistent, and coherent, since it does not require any preliminary knowledge about collisional parameters.

II. LINE-SHAPE THEORY

The profile $S(\omega)$ of a spectral line is given by the Fourier transform of the dipole correlation function, $\Phi(t)$:

$$S(\omega) = \frac{1}{\pi} \text{Re} \int_0^\infty dt \Phi(t) e^{-i\omega t}. \quad (2)$$

Within the classical approach given by Rautian and Sobel'man [10], the dipole correlation function can be evaluated by integrating the dipole distribution function $F(t, \mathbf{v})$, over all possible absorbers' velocities, \mathbf{v} , as follows:

$$\Phi(t) = \int d^3\mathbf{v} F(t, \mathbf{v}). \quad (3)$$

Combining Eqs. (2) and (3), the line-shape function can be written as

$$S(\omega) = \text{Re} \int d^3\mathbf{v} \mathcal{F}(\omega, \mathbf{v}), \quad (4)$$

where $\mathcal{F}(\omega, \mathbf{v})$ is the Fourier transform of dipole distribution function, which has the meaning of a complex line-shape function for the group of molecules with velocity \mathbf{v} . In turn, $\mathcal{F}(\omega, \mathbf{v})$ satisfies the Boltzmann kinetic equation that, in the $\mathbf{k} - \omega$ space, can be written as

$$\frac{1}{\pi} F(0, \mathbf{v}) = -i(\omega - \omega_0 - \mathbf{k} \cdot \mathbf{v}) \mathcal{F}(\omega, \mathbf{v}) - \hat{S}_{\text{coll}} \mathcal{F}(\omega, \mathbf{v}), \quad (5)$$

where ω_0 is the rest transition frequency and \mathbf{k} is the wave vector of the absorbed light with magnitude $k = \omega_0/c$. We assume that the initial dipole distribution function is the Maxwell-Boltzmann function:

$$F(0, \mathbf{v}) = f_m(\mathbf{v}) = \left(\frac{1}{\pi v_m^2} \right)^{3/2} \exp\left(-\frac{v^2}{v_m^2}\right), \quad (6)$$

where $v_m = \sqrt{2k_B T/m_A}$ is the most probable speed of absorbing molecules with mass m_A and $v = |\mathbf{v}|$. If we assume that the velocity-changing collisions and dephasing collisions are correlated then the collision operator \hat{S} can be split in three operators:

$$\hat{S}_{\text{coll}} = \hat{S}_D + \hat{S}_{\text{VC}} + \hat{S}_{\text{VCD}}, \quad (7)$$

where \hat{S}_D is the purely dephasing collision operator, \hat{S}_{VC} is the purely velocity-changing collision operator and \hat{S}_{VCD} is the collision operator that takes into account the physical correlation between the two types of collisions, namely, the occurrence of collisions that jointly provide a variation of

molecular velocity and a dephasing of the molecular dipole. In the impact approximation, the dephasing collision operator can be decomposed into its real and imaginary parts as follows [11]:

$$\hat{S}_D \mathcal{F}(\omega, \mathbf{v}) = -[\Gamma_D(v) + i\Delta_D(v)] \mathcal{F}(\omega, \mathbf{v}), \quad (8)$$

$\Gamma_D(v)$ and $\Delta_D(v)$ being the collisional width and shift, respectively. The velocity-changing collision operator \hat{S}_{VC} is defined as follows:

$$\begin{aligned} \hat{S}_{\text{VC}} \mathcal{F}(\omega, \mathbf{v}) = & - \int d^3\mathbf{v}' A(\mathbf{v}' \leftarrow \mathbf{v}) \mathcal{F}(\omega, \mathbf{v}) \\ & + \int d^3\mathbf{v}' A(\mathbf{v} \leftarrow \mathbf{v}') \mathcal{F}(\omega, \mathbf{v}'). \end{aligned} \quad (9)$$

It is clear that the form of \hat{S}_{VC} is determined by the collisional kernel $A(\mathbf{v} \leftarrow \mathbf{v}')$, which gives the rate of molecules transferred into the cell at \mathbf{v} from the cell centered at \mathbf{v}' . We now consider two models for the collisional kernel, providing different forms for the collision operators \hat{S}_{VC} and \hat{S}_{VCD} .

A. Keilson-Storer model

The collisional kernel proposed by Keilson and Storer (KS) is given by [12]

$$\begin{aligned} A(\mathbf{v} \leftarrow \mathbf{v}') &= \nu_{\text{VC}} A_{\text{KS}}(\mathbf{v} \leftarrow \mathbf{v}'; \alpha) \\ &= \nu_{\text{VC}} \left(\frac{1}{\pi(1-\alpha^2)v_m^2} \right)^{3/2} \exp\left[-\frac{(\mathbf{v} - \alpha\mathbf{v}')^2}{(1-\alpha^2)v_m^2} \right], \end{aligned} \quad (10)$$

where ν_{VC} is the frequency of velocity-changing collisions and α is the memory parameter that must obey the inequality $0 \leq \alpha < 1$, in order to give $A(\mathbf{v} \leftarrow \mathbf{v}')$ real and to drive the distribution to equilibrium. The properties of the KS kernel are discussed by Snider in Ref. [13]. Here we limit the discussion to the main features. Obviously, the KS kernel is normalized as any other probability distribution function. Therefore, the following equation holds:

$$\int d^3\mathbf{v} A_{\text{KS}}(\mathbf{v} \leftarrow \mathbf{v}'; \alpha) = 1. \quad (11)$$

The memory parameter α is related to the average change of the velocity caused by a single collision, namely, $\langle \mathbf{v}' \rangle = \alpha \langle \mathbf{v} \rangle$, \mathbf{v}' and \mathbf{v} being the velocity after and before a collision, respectively. Therefore, $\alpha = 0$ means that after each collision the velocity is completely uncorrelated with respect to the velocity before the collision. On the other hand, the limit $\alpha \rightarrow 1$ can be treated as a Brownian motion, whereas an individual collision has a negligible effect on the velocity but collectively they are significant. Finally, it can be shown that the KS kernel has no effect on the Maxwell-Boltzmann velocity distribution, since the following equation holds:

$$\int d^3\mathbf{v}' A_{\text{KS}}(\mathbf{v} \leftarrow \mathbf{v}'; \alpha) f_m(\mathbf{v}') = f_m(\mathbf{v}). \quad (12)$$

Substituting Eq. (10) into Eq. (9), it can be shown that the velocity-changing collision operator becomes

$$\begin{aligned} \hat{S}_{\text{VC}} \mathcal{F}(\omega, \mathbf{v}) &= -\nu_{\text{VC}} \mathcal{F}(\omega, \mathbf{v}) \\ &+ \nu_{\text{VC}} \int d^3\mathbf{v}' A_{\text{KS}}(\mathbf{v} \leftarrow \mathbf{v}'; \alpha) \mathcal{F}(\omega, \mathbf{v}'). \end{aligned} \quad (13)$$

The collision operator \hat{S}_{VCD} , which takes into account the partial correlation between velocity-changing and dephasing collisions, can be written as [14]

$$\begin{aligned} & \hat{S}_{\text{VCD}}\mathcal{F}(\omega, \mathbf{v}) \\ &= -[\Gamma_{\text{VD}}(v) + i\Delta_{\text{VD}}(v)]\mathcal{F}(\omega, \mathbf{v}) - \nu_{\text{VCD}} \\ & \quad - [\Gamma_{\text{VD}}(v) + i\Delta_{\text{VD}}(v)] \\ & \quad \times \left[\mathcal{F}(\omega, \mathbf{v}) - \int d^3\mathbf{v}' A_{\text{KS}}(\mathbf{v} \leftarrow \mathbf{v}'; \alpha) \mathcal{F}(\omega, \mathbf{v}') \right], \end{aligned} \quad (14)$$

where $\Gamma_{\text{VD}}(v)$ and $\Delta_{\text{VD}}(v)$ represent the pressure width and shifting caused by VCD-type collisions and ν_{VCD} is the associated frequency. Assuming $\Gamma(v) = \Gamma_{\text{D}}(v) + \Gamma_{\text{VD}}(v)$, and $\Delta(v) = \Delta_{\text{D}}(v) + \Delta_{\text{VD}}(v)$, we can define the parameter $\eta = \Gamma_{\text{VD}}(v)/\Gamma(v) = \Delta_{\text{VD}}(v)/\Delta(v)$ that is the fraction of collisional broadening and shifting provided from \hat{S}_{VCD} .

Therefore, combining the contributions of the collision operators given by Eqs. (8), (13), and (14), the kinetic Boltzmann equation becomes

$$\begin{aligned} \frac{1}{\pi} f_m(\mathbf{v}) &= [\Gamma(v) + \tilde{\nu}(v)]\mathcal{F}(\omega, \mathbf{v}) \\ & \quad - i[\omega - \omega_0 - \mathbf{k} \cdot \mathbf{v} - \Delta(v)]\mathcal{F}(\omega, \mathbf{v}) \\ & \quad - \tilde{\nu}(v) \int d^3\mathbf{v}' A_{\text{KS}}(\mathbf{v} \leftarrow \mathbf{v}'; \alpha) \mathcal{F}(\omega, \mathbf{v}'), \end{aligned} \quad (15)$$

where $\tilde{\nu}(v) = (\nu_{\text{VC}} + \nu_{\text{VCD}}) - \eta[\Gamma(v) + i\Delta(v)]$ is the effective speed-dependent velocity-changing collision frequency. Moreover, the quantity $\nu_{\text{VC}} + \nu_{\text{VCD}}$, which is the total frequency of velocity-changing collision, may be connected to the diffusion coefficient D for the active species in a buffer gas by [12]

$$D = \frac{k_B T}{2\pi m_A (\nu_{\text{VC}} + \nu_{\text{VCD}})(1 - \alpha)}. \quad (16)$$

Therefore, the diffusion collision frequency is related to the total velocity-changing collision frequency by means of the expression $\nu_{\text{diff}} = (\nu_{\text{VC}} + \nu_{\text{VCD}})(1 - \alpha)$. The solution of Eq. (15), combined with Eq. (4), leads to the partially correlated speed-dependent Keilson-Storer profile (pCSDKSP).

In order to solve Eq. (15), we have adopted the iterative method proposed by Nienhuis [15,16] with some variations, as shown by Wcislo *et al.* [17]. In this approach, the exact solution of the kinetic equation is given by $\mathcal{F}(\omega, \mathbf{v}) = \lim_{n \rightarrow \infty} \mathcal{F}^{(n)}(\omega, \mathbf{v})$, where the distribution $\mathcal{F}^{(n)}(\omega, \mathbf{v})$ can be obtained from $\mathcal{F}^{(n-1)}(\omega, \mathbf{v})$ using the relationship

$$\begin{aligned} \mathcal{F}^{(n)}(\omega, \mathbf{v}) &= L(\omega, \mathbf{v}) \times \left[\frac{1}{\pi} f_m(\mathbf{v}) + \tilde{\nu}(v) \right. \\ & \quad \left. \times \int d^3\mathbf{v}' A_{\text{KS}}(\mathbf{v} \leftarrow \mathbf{v}'; \alpha) \mathcal{F}^{(n-1)}(\omega, \mathbf{v}') \right], \end{aligned} \quad (17)$$

where

$$L(\omega, \mathbf{v}) = \frac{1}{\Gamma(v) + \tilde{\nu}(v) - i[\omega - \omega_0 - \mathbf{k} \cdot \mathbf{v} - \Delta(v)]}. \quad (18)$$

The initial distribution function $\mathcal{F}^{(0)}(\omega, \mathbf{v})$ determines the rapidity of convergence, but it has no influence on the final result. In this work, we set $\mathcal{F}^{(0)}(\omega, \mathbf{v}) = 0$. This iterative

scheme works very well as long as the following condition is satisfied:

$$\left| \tilde{\nu}(v) \int d^3\mathbf{v}' A_{\text{KS}}(\mathbf{v} \leftarrow \mathbf{v}'; \alpha) L(\omega, \mathbf{v}) \right| < 1, \quad (19)$$

so that $\mathcal{F}^{(n)}(\omega, \mathbf{v})$ may be approximated by a limited number of steps. This is certainly the case in the far wings but near the line center ω_0 the contribution of $\Gamma(v) + \tilde{\nu}(v)$ is crucial. In fact, in the Doppler limit ($\Gamma_{av} < 0.1k v_m$, being Γ_{av} the average collisional width over absorber speed), the iterative scheme reported in Eq. (17) fails. To ensure the stability of the iterative perturbation process and to control its convergence we have implemented the new iterative approach of Wcislo *et al.* in Ref. [17]. In the kinetic Boltzmann equation, Eq. (5), a nonphysical parameter, Γ_n , has been introduced as follows:

$$\begin{aligned} \frac{1}{\pi} F(0, \mathbf{v}) &= \Gamma_n - i(\omega - \omega_0 - \mathbf{k} \cdot \mathbf{v})\mathcal{F}(\omega, \mathbf{v}) \\ & \quad - (\Gamma_n + \hat{S}_{\text{coll}})\mathcal{F}(\omega, \mathbf{v}). \end{aligned} \quad (20)$$

Now, with a simple algebraic manipulation, we obtain a modified iterative scheme:

$$\begin{aligned} \mathcal{F}^{(n)}(\omega, \mathbf{v}) &= \frac{1}{\Gamma_n - i[\omega - \omega_0 - \mathbf{k} \cdot \mathbf{v}]} \times \left\{ \frac{1}{\pi} f_m(\mathbf{v}) \right. \\ & \quad + [\Gamma_n - \Gamma(v) - \tilde{\nu}(v) - i\Delta(v)]\mathcal{F}^{(n-1)}(\omega, \mathbf{v}) \\ & \quad \left. + \tilde{\nu}(v) \int d^3\mathbf{v}' A_{\text{KS}}(\mathbf{v} \leftarrow \mathbf{v}'; \alpha) \mathcal{F}^{(n-1)}(\omega, \mathbf{v}') \right\}. \end{aligned} \quad (21)$$

The stability and convergence is guaranteed by the fact that the size of the term,

$$\int d^3\mathbf{v}' \frac{A_{\text{KS}}(\mathbf{v} \leftarrow \mathbf{v}'; \alpha)}{\Gamma_n - i[\omega - \omega_0 - \mathbf{k} \cdot \mathbf{v}]}, \quad (22)$$

is regulated by the fixed value of Γ_n .

From a computational point of view, the three-dimensional integration over the space of velocity of Eqs. (15) and (21) can be reduced to two dimensions using cylindrical coordinates (v_r, v_z, ϕ) in which the z axis is parallel to the wave vector \mathbf{k} ; this choice makes the distribution function $\mathcal{F}(\omega, \mathbf{v})$ independent from the angle ϕ . Therefore, we obtain that $d^3\mathbf{v}$ can be substituted by $2\pi v_r dv_z dv_r$, where v_z is the component of \mathbf{v} on the z axis, v_r is the projection of \mathbf{v} on the radial plane, and $v = \sqrt{v_r^2 + v_z^2}$.

B. Rautian-Sobel'man model

A closed solution of the Boltzmann transport equation, Eq. (5), is obtained adopting the velocity-changing collisional operator \hat{S}_{VC} proposed by Rautian and Sobel'man [10] and generalized by Ciurylo *et al.* in Ref. [14], in the case of statistical correlation between velocity-changing and dephasing collisions as follows:

$$\begin{aligned} \hat{S}_{\text{VC}}\mathcal{F}(\omega, \mathbf{v}) &= -\nu_{\text{VC}}[\epsilon \hat{A}_H + (1 - \epsilon) \hat{A}_S]\mathcal{F}(\omega, \mathbf{v}), \\ \hat{S}_{\text{VCD}}\mathcal{F}(\omega, \mathbf{v}) &= -\{\nu_{\text{VCD}} - \eta[\Gamma(v) + i\Delta(v)]\} \\ & \quad \times [\epsilon \hat{A}_H + (1 - \epsilon) \hat{A}_S]\mathcal{F}(\omega, \mathbf{v}). \end{aligned} \quad (23)$$

Here, the η parameter is identical to that defined in the previous section. This approach assumes that a fraction ϵ of

the velocity-changing collisions is hard, in which the velocities are completely uncorrelated, while the remaining part $(1 - \epsilon)$ is soft. The hard and soft collision operators, \hat{A}_H and \hat{A}_S , can be written as [14]:

$$\begin{aligned}\hat{A}_H \mathcal{F}(\omega, \mathbf{v}) &= \mathcal{F}(\omega, \mathbf{v}) - f_m(\mathbf{v}) \int d^3 \mathbf{v}' \mathcal{F}(\omega, \mathbf{v}'), \\ \hat{A}_S \mathcal{F}(\omega, \mathbf{v}) &= -\nabla_v(\mathbf{v} \mathcal{F}(\omega, \mathbf{v})) - \frac{k_B T}{m_A} \nabla_v^2 \mathcal{F}(\omega, \mathbf{v}).\end{aligned}\quad (24)$$

In the dimensionless variables $\tau = \omega_D t$, $x = v/v_m$, $u = (\omega - \omega_0)/\omega_D$, $g(x) = (\Gamma_{av}/\omega_D) B(x v_m, m)$, $d(x) = (\Delta_{av}/\omega_D) B(x v_m, n)$, being Δ_{av} the average collisional shift over absorber speed, $z_{\text{diff}} = v_{\text{diff}}/\omega_D$, $\omega_D = k v_m$ being the Doppler width (half width at $1/e$ of the maximum), the solution of the Boltzmann transport equation provides the partially correlated speed-dependent hard- and soft-collision profile (pCSDHSCP):

$$S_{\text{pCSDHSCP}}(\omega) = \text{Re} \left[\frac{G(u)}{1 - \pi H(u)} \right], \quad (25)$$

where $G(u)$ and $H(u)$ are the Fourier Transform of $K_1(\tau)$ and $K_2(\tau)$, respectively:

$$G(u) = \frac{4}{\pi^{3/2}} \int_0^\infty d\tau K_1(\tau) e^{i u \tau}, \quad (26a)$$

$$H(u) = \frac{4}{\pi^{3/2}} \int_0^\infty d\tau K_2(\tau) e^{i u \tau}. \quad (26b)$$

The K 's function are given by:

$$K_1(\tau) = \int_0^\infty dx J(x, \tau), \quad (27a)$$

$$K_2(\tau) = \int_0^\infty dx h(x) J(x, \tau), \quad (27b)$$

where $J(x, \tau)$:

$$\begin{aligned}J(x, \tau) &= x^2 e^{-x^2} \text{sinc}[x(1 - e^{-s(x)\tau})/s(x)] \\ &\times \exp\{-[2s(x)\tau - 3 + 4e^{-s(x)\tau} - e^{-2s(x)\tau}]/[4s(x)^2]\} \\ &\times \exp\{-[h(x) + g(x) + id(x)]\tau\}.\end{aligned}\quad (28)$$

Finally, $h(x)$ and $s(x)$ are the effective frequency of hard and soft collisions, respectively, modified by a partial correlation between dephasing and velocity-changing collisions:

$$h(x) = \epsilon \{z_{\text{diff}} - \eta [g(x) + id(x)]\}, \quad (29a)$$

$$s(x) = (1 - \epsilon) \{z_{\text{diff}} - \eta [g(x) + id(x)]\}. \quad (29b)$$

We underline that setting $\eta = 0$ we obtain the speed-dependent Rautian-Sobelman profile [10]. Furthermore, the corresponding partially correlated speed-dependent hard-collision profile (pCSDHCP), proposed by Pine in Ref. [18], is obtained setting $\epsilon = 1$. Finally, the uncorrelated speed-dependent hard-collision profile (SDHCP) [19] and speed-dependent soft-collision profile [11] can be obtained setting $\eta = 0$ with $\epsilon = 1$ and $\epsilon = 0$, respectively.

C. Speed dependence of collisional parameters

In the formalism developed by Berman and Pickett [20,21] the collisional parameters are supposed to have a power-law dependence on the relative speed of the absorber-perturber system, with an exponent determined by the molecular interaction potential, which in turn is approximated by an inverse power form, namely, $V(r) \propto 1/r^q$. The statistical average over the relative speeds provide the following expression for the collisional width and shift [22]:

$$\Gamma(v) = \frac{\Gamma_{av}}{(1 + \mu)^{m/2}} M \left[-\frac{m}{2}, \frac{3}{2}, -\mu \left(\frac{v}{v_m} \right)^2 \right] = \Gamma_{av} B(v, m), \quad (30)$$

$$\begin{aligned}\Delta(v) &= \frac{\Delta_{av}}{(1 + \mu)^{n/2}} M \left[-\frac{n}{2}, \frac{3}{2}, -\mu \left(\frac{v}{v_m} \right)^2 \right] = \Delta_{av} B(v, n), \\ \mu &= \frac{m_p}{m_A}, \quad m = \frac{q-3}{q-1}, \quad n = -\frac{3}{q-1}\end{aligned}\quad (31)$$

Here, $M(a, b, z)$ is the confluent hypergeometric function, m_p is the perturber mass, while Γ_{av} and Δ_{av} show a linear dependence on the pressure, namely, $\Gamma_{av} = \gamma_{av} p$, $\Delta_{av} = \delta_{av} p$.

III. SIMULATED ABSORPTION SPECTRA BY MEANS OF THE pCSDKSP

The light absorption in a gaseous sample is ruled by the well-known Lambert-Beer law:

$$P(\omega) = P_0 \exp[-A \cdot S(\omega)], \quad (32)$$

where A represents the integrated absorbance, P_0 the incident power (which can be frequency dependent), $P(\omega)$ the transmitted power at the angular frequency ω , and $S(\omega)$ the line shape function. The iterative scheme of Eqs. (15) and (21) was implemented under the MATLAB environment. The stopping criterion, adopted for all the calculated spectra, is given by $|S^{(n)}(\omega) - S^{(n-1)}(\omega)| < 10^{-16}$. The double integral was calculated by means of the Boole integration rule. More particularly, the integral over v_z was done using 2409 points in the interval between $-5v_m$ and $5v_m$, while the integral over v_r was done using 1205 points in the range from 0 to $5v_m$. The comparison between speed-dependent hard-collision profiles as calculated using the iterative method, setting $\alpha = 0$, and the more conventional approach of Eq. (25) with $\eta = 0$ and $\epsilon = 1$, using comparable numbers of points in the speed grid, shows a maximum relative deviation (at the peak absorption) of about 6×10^{-7} at any pressures (namely, for a Γ_{av}/ω_D ratio between 0.0026 and 0.1225). The spectroscopic parameters were set at the values reported in the literature [5,28]. Similarly, the Doppler width was fixed at the value of 342.9598 MHz that is retrieved for $T = 273.16$ K and $k = 2\pi \tilde{\nu}_0$, where $\tilde{\nu}_0 = 7199.1032 \text{ cm}^{-1}$ is the wave number of the $4_{4,1} \rightarrow 4_{4,0}$ vibration-rotation transition of the $\text{H}_2^{18}\text{O } \nu_1 + \nu_3$ band. This is the line on which the most accurate spectroscopic determination of the Boltzmann constant was performed [3]. The collisional-broadening coefficient γ_{av} was fixed at the value of 105 kHz/Pa with a hypergeometric speed dependence characterized by $m = 0.5$ [see Eq. (31)], according to recent

findings [5]. The speed dependence of pressure shift was not considered. The memory parameter, α , was set at the value of 0.17, as recently calculated by Ngo *et al.* in Ref. [8] by means of classical molecular dynamics simulations on self-colliding water molecules. The diffusion frequency is determined from the experimental value of the water self-diffusion coefficient, as reported in Ref. [23], after proper scaling with the temperature ($D = 1.93 \text{ cm}^2 \text{ s}^{-1} \text{ Pa}$), thus providing a diffusion frequency per unit pressure, β_{diff} , of 12.076 kHz/Pa. Finally, the choice of the correlation parameter, η , was done so as to have a positive effective velocity-changing collision frequency, which means $\eta \leq v_{\text{diff}}/[(1-\alpha)\Gamma_{av}]$. In our simulations we set $\eta = 0.1$. A variety of pCSDKSPs in the pressure range between 10 to 467 Pa were calculated. Each spectrum consists of 3000 points in a frequency range of 3 GHz. A random noise was added to the simulated spectra to reproduce the experimental situation of Ref. [3] (signal-to-noise ratio, S/N , of about 10 000, measured on the maximum transmitted signal). For each of the ten selected pressure values, 100 spectra were simulated.

IV. GLOBAL FITTING PROCEDURE

The multispectrum fitting procedure (MSFP) was developed in order to analyze simultaneously absorption spectra across the entire pressure range, following the pioneering work of Benner *et al.* [24]. In this approach physical relations between spectroscopic parameters are incorporated in a global function, $\chi_G^2(\mathbf{X}, \mathbf{Y}, \mathbf{W}; \mathbf{p}_G)$. Here, the matrices \mathbf{X} , \mathbf{Y} , and \mathbf{W} , whose size is $N \times M$, represent experimental data and statistical weights, N being the number of points for each spectrum and M the number of spectra corresponding to different pressures. More specifically, y_{ij} is the transmitted signal of the j th spectrum at the laser frequency x_{ij} , while its uncertainty is $1/\sqrt{w_{ij}}$. The parameters' vector, \mathbf{p}_G , consists of elements of two different types: Those shared among different spectra, such as the pressure broadening and shifting coefficients, the correlation parameter, the velocity-changing collision frequency per unit pressure (β), and those that are characteristic of individual spectra, namely, the integrated absorbance, A_j , and the baseline parameters, P_{0j} and P_{1j} . It is worth noting that, even though the simulated spectra had a constant baseline as a function of the frequency, a slope parameter (P_{1j}) was considered in the fitting procedure. Obviously, the size of \mathbf{p}_G depends on the number of spectra entering into the global analysis and it is reduced when simplified line shape models are used. We implemented the MSFP over 10 spectra at different pressure values, adopting the following models: SDHCP, pCSDHCP, and pCSDHSCP. In the simplest case of the SDHCP model, the total number of free parameters is 37, of which 7 are shared among the spectra: ω_0 , γ_{av} , ω_D , δ_{av} , m , n , and β . Instead, for the most sophisticated case, given by the pCSDHSCP, we have 9 shared parameters, adding η and ϵ to those listed above, for a total of 39 free parameters. The MSFP procedure was implemented under the MATLAB environment, using a Levenberg-Marquardt algorithm for the minimization of the global χ -square, thus providing the best estimate of \mathbf{p}_G . For a more detailed description of the global fitting approach, also regarding the calculation of the statistical uncertainty of the retrieved parameters, the reader is referred to Ref. [25].

V. RESULTS AND DISCUSSION

The simulated spectra were globally analyzed by means of the MSFP. A variety of semiclassical models were implemented and tested in the global fitting procedure. As a first step, we tested the speed-dependent Voigt model. As expected, the results were significantly away from the set point, being 51 ppm smaller.

Since the memory parameter of the KS kernel was set to $\alpha = 0.17$ in the numerically simulated spectra, the physical situation is expected to be close to the one of the hard-collision model (namely, $\alpha = 0$); as a consequence, we decided to test the SDHCP and pCSDHCP models. Furthermore, we implemented the pCSDHSCP, this latter model accounting for both hard and soft collisions, as already explained in Sec. II B. In Fig. 1, typical residuals are shown, resulting from the application of the fitting routine with the three line-shape models. In each case, the residuals do not show any particular deviation between theory and experiment, their root-mean-square (rms) values being roughly coincident with the simulated noise level. A very small structure around the line-center frequency is visible only for the pCSDHCP. Obviously, the same level of agreement is not found when applying the speed-dependent Voigt model, the rms value being of the order of 1 mV. Despite the excellent results of Fig. 1, as observed at any pressure, the physical difference between velocity-changing collisional mechanisms, which is captured by the adopted semiclassical models, as compared to the Keilson-Storer model, provides some amount of inaccuracy in the determination of the Doppler width. In fact, after the global analysis of ten simulated spectra across the entire pressure range, the relative deviation between retrieved and expected Doppler widths, given by $(\omega_{\text{Dretr}} - \omega_D)/\omega_D$, was 12.5, 14.7, and 24.0 ppm, respectively, for the SDHCP, pCSDHCP, and pCSDHSCP. On the other hand, the relative statistical uncertainty, defined as $\sigma_D/\omega_{\text{Dretr}}$ (where σ_D is the internal error resulting from the MSFP procedure) was 6.7, 7.5, and 11.5 ppm, respectively. From these first results, it seems clear that the best performance in terms of precision and accuracy is ensured by the speed-dependent hard-collision profile. Surprisingly, the pCSDHSCP model, which was expected to better reproduce the physical situation of the simulated spectra, provided the worst results. The explanation must be sought in the strong statistical correlation between the Doppler width and other shared parameters, namely, η , m , and ϵ , as clearly evidenced in Fig. 2. From this plot, it appears that the best performance is provided by the pCSDHCP. Nevertheless, this latter model shows some limitations in the residuals, as already discussed above. Furthermore, it provides bad estimates for β_{diff} and η with no physical meaning, both values being negative. Therefore, the SDHCP model has to be preferred because of the most accurate performance in the retrieval of the Doppler width, in conjunction to a reduced number of free parameters and to the realistic value that is returned for the velocity-changing collision frequency. The results that will be discussed in the remaining part of this article refer to the speed-dependent hard-collision model and are aimed to investigate the ultimate performance of this profile.

The discrepancy in Doppler width retrieval resulting from the global analysis of a restricted number of spectra (ten, in

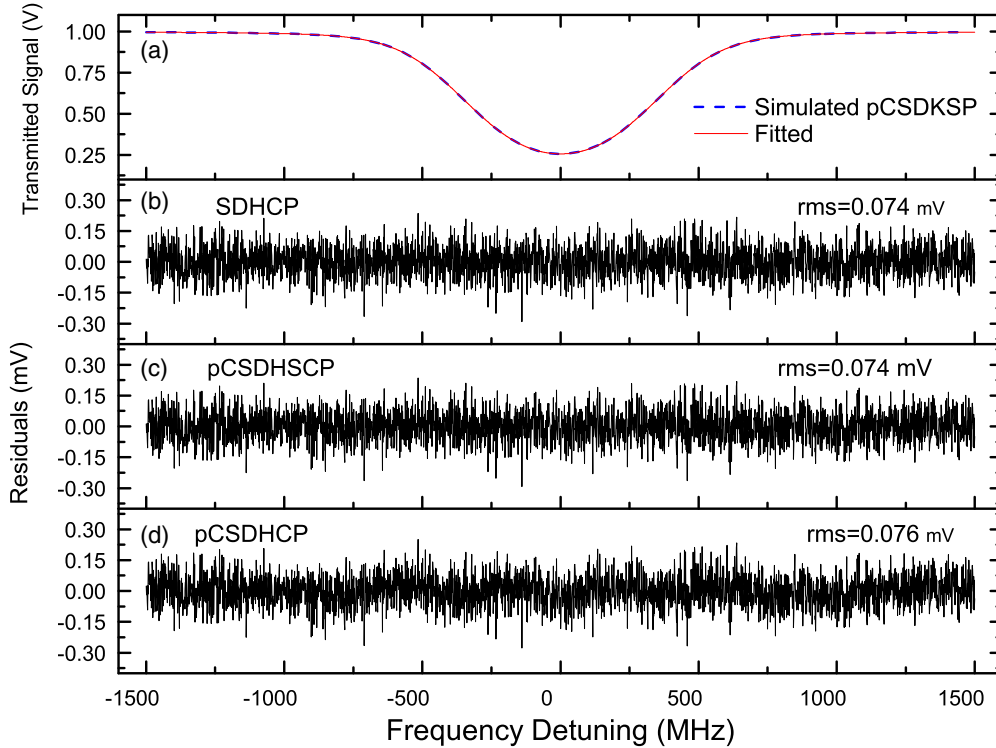


FIG. 1. (Color online) Results of the multispectrum fitting procedure performed on simulated spectra with a signal-to-noise ratio of 10 000, using different semiclassical models: (a) Simulated absorption spectrum with pCSDKSP (dotted line) together with the best-fit resulting with MSFP (full line); (b) speed-dependent hard-collision profile; (c) partially correlated speed-dependent hard-collision profile; (d) partially correlated speed-dependent hard- and soft-collision profile. The upper plot shows the comparison between an example spectrum and its interpolation with the SDHCP model.

the present situation) can be ascribed to two different reasons: statistical fluctuation and model limitation. As for the first source of discrepancy, we remind that the simulated spectra exhibit a signal-to-noise ratio of 10 000; therefore, it is likely that the global analysis of a small number of spectra provides a shifted value for the Doppler width. On the other hand, the SDHCP model is based upon a collision kernel that is different from that of the pCSDKSP. Such a difference can

be a source of discrepancy, which can be named as *model discrepancy*. The *statistical discrepancy*, in principle, can be strongly reduced by analyzing a much larger number of spectra. In Fig. 3, we report the obtained levels of accuracy and precision in the determination of ω_D as a function of the number of repeated datasets that are sequentially analyzed. We remind that each dataset consists of ten simulated spectra in the pressure interval between 67 and 467 Pa. The ω_D value is given by the weighted mean of the values resulting from the global analysis that is repeated over a given number of datasets. Similarly, the statistical uncertainty is given by the error of the weighed mean. In each plot, the red line is obtained from the MSFP procedure when it is applied to ten simulated spectra without the addition of noise. It can be noted that the weighted mean over 80 datasets gives a sub-ppm precision, while the inaccuracy amounts to about 7 ppm, both being very close to those obtained from simulated spectra without noise.

A comparison between the results obtained from individual and global fits is shown in Fig. 4. Each red point represents a ω_D value resulting from the application of the MSFP to a dataset of ten simulated spectra, while each black point is the weighted mean of the Doppler widths as retrieved from the single spectrum fitting procedure (SSFP) applied to the ten spectra of each dataset. In total, 100 points are plotted either for the results of the MSFP or for the SSFP procedure, involving the same number of simulated spectra (1000, in total). It is worth noting that the standard deviation of ω_D is 0.026 MHz for the SSFP, while it amounts to 0.0021 MHz for the MSFP.

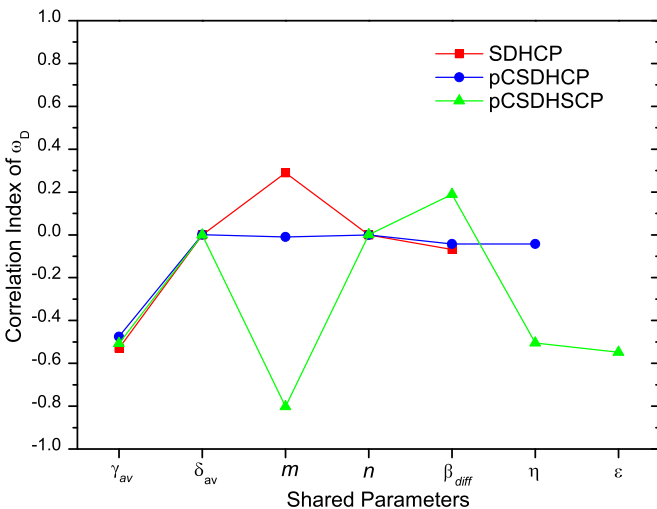


FIG. 2. (Color online) Statistical correlation index of Doppler width with respect to the other spectroscopic parameters.

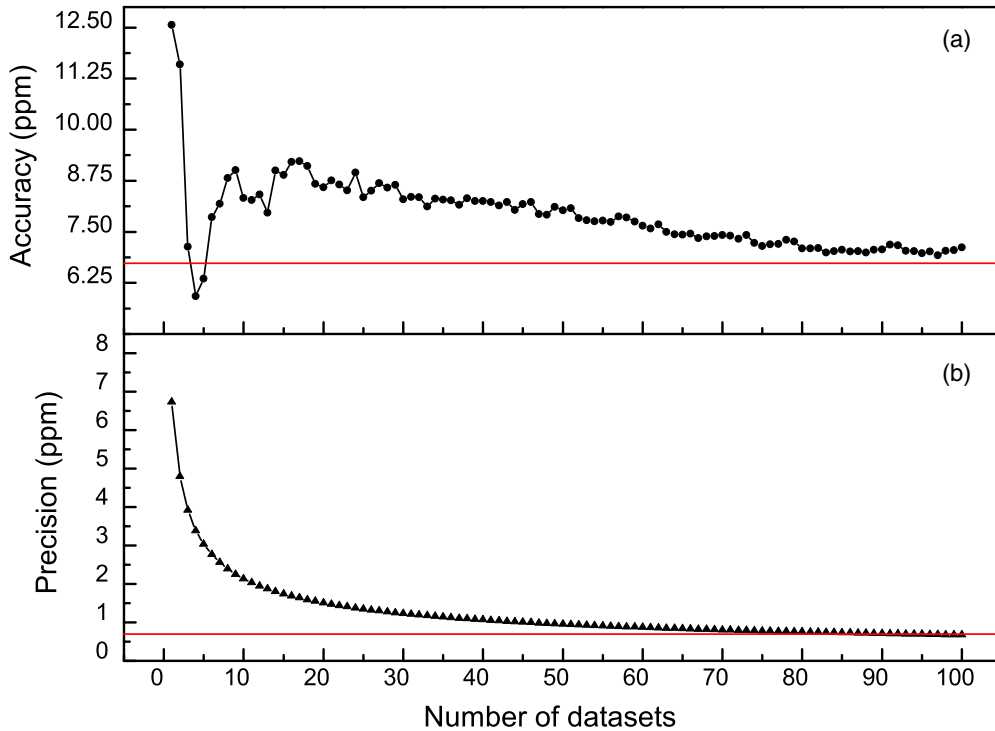


FIG. 3. (Color online) Behavior of accuracy (a) and precision (b) of Doppler width estimation as function of the number of datasets. The red-lines represent the values obtained from the MSFP of single dataset with no-noise spectra.

Hence, the advantage of the global approach is clear: the gain in precision, with respect to individual fits, is larger than a factor of 10. The shift with respect to the expected value amounts to +7 and -21 ppm, respectively, for the MSFP and the SSFP procedure. Also in this, the advantage of the global approach is evident.

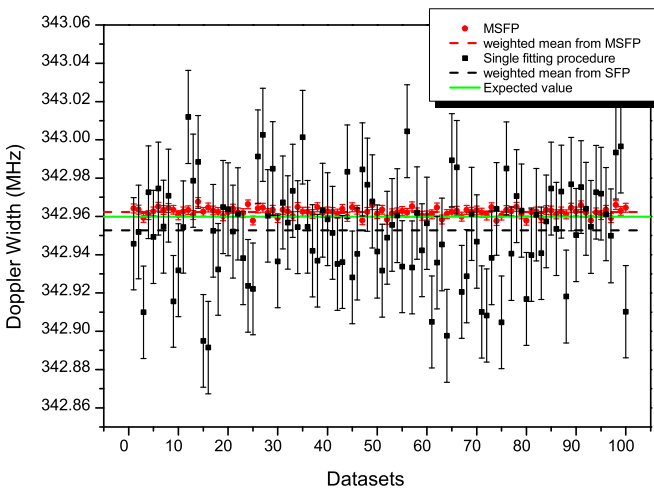


FIG. 4. (Color online) Comparison between the single fitting procedure (SFP) and multispectra fitting procedure (MSFP) in the retrieved Doppler width. Both the procedure has been achieved on 100 datasets of 10 spectra for each one. The red dashed line represents the weighted mean obtained with MSFP; the black line represents the weighted mean with SFP. The green line represents the value that is set in the numerical simulations.

To further investigate the accuracy problem, we repeated the global analysis of simulated spectra changing the pressure interval. In particular, the lower limit was kept constant (10 Pa) while the upper limit was reduced from 470 Pa down to 100 Pa. Figure 5 shows the trends obtained for precision and accuracy levels. It is interesting to note that the precision gets slightly worse, while the determination of ω_D results to be more and more accurate. In particular, the pressure range between 10 and 150 Pa for the simulated spectra gives a precision of 0.42 ppm and a systematical deviation as small as 0.75 ppm.

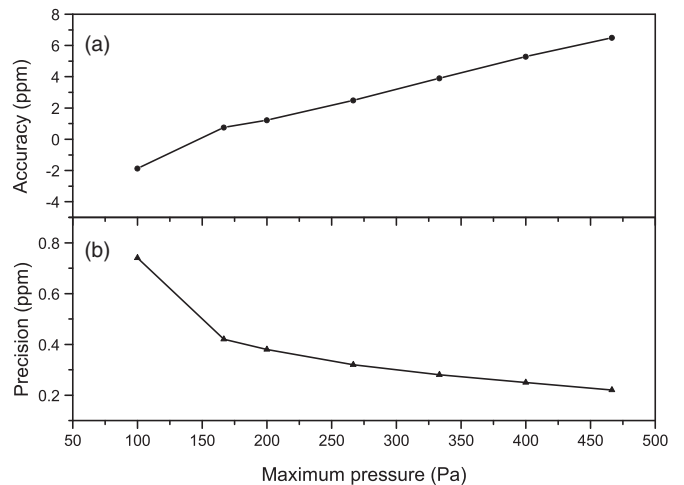


FIG. 5. Behavior of (a) accuracy and (b) precision of Doppler width as function of the maximum pressure involved in the MSFP.

VI. CONCLUSIONS

In conclusion, our study clearly demonstrates that the achievement of the ppm level for both the statistical uncertainty and for the uncertainty associated to the line-shape model is a realistic possibility of which DBT can really benefit for being competitive with more consolidated techniques, like acoustic gas thermometry [26]. To this end, the global fitting approach appears to be an indispensable tool, also providing strong elements for the selection of most appropriate line-shape models. On the other hand, it allows one to use rather sophisticated profiles even without the precise knowledge of key parameters such as the pressure-broadening coefficient or the velocity-changing collision frequency. Among the tested models, the best performance in terms of precision and accuracy in the retrieval of the Doppler width is obtained by the speed-dependent hard-collision profile. Our study is limited to 1000 simulated spectra, obtained by using the partially correlated speed-dependent Keilson-Storer model to the best of our knowledge, this latter turns out to be the most realistic model for a pure water line in the infrared region, capable of capturing the various collisional perturbations of the isolated line. Unfortunately, we cannot quantify possible inaccuracies

(in the Doppler widths) coming from the capability of the pCSDKSP to reproduce real water spectra. To this end, it might be useful to repeat our study by using more sophisticated kernels, such as the cusp kernels and their superpositions [27]. Also, a comparison between the profiles based upon the Keilson-Storer kernel and the cusp kernels would be of great importance. These possibilities are being considered for future work. When it comes to the simplified models, we cannot exclude that the pCSDHCP and pCSDHSCP models can provide the same performance as compared to the SDHCP, using a much larger number of spectra. The SDHCP model gives a Doppler width with type A and B uncertainties of 0.42 and 0.75 ppm, respectively.

ACKNOWLEDGMENTS

This research was carried out in the framework of the European Metrology Research Programme (EMRP), Project No. SIB01-REG4 (responsible, Livio Gianfrani) within the InK project (Implementing the new Kelvin, coordinated by Graham Machin). The EMRP is jointly funded by the EMRP participating countries within EURAMET and the European Union.

-
- [1] C. Daussy, M. Guinet, A. Amy-Klein, K. Djerroud, Y. Hermier, S. Briaudeau, C. J. Bordé, and C. Chardonnet, *Phys. Rev. Lett.* **98**, 250801 (2007).
 - [2] G. Casa, A. Castrillo, G. Galzerano, R. Wehr, A. Merlone, D. Di Serafino, P. Laporta, and L. Gianfrani, *Phys. Rev. Lett.* **100**, 200801 (2008).
 - [3] L. Moretti, A. Castrillo, E. Fasci, M. D. De Vizia, G. Casa, G. Galzerano, A. Merlone, P. Laporta, and L. Gianfrani, *Phys. Rev. Lett.* **111**, 060803 (2013).
 - [4] M. J. T. Milton, R. Davis, and N. Fletcher, *Metrologia* **51**, R21 (2014).
 - [5] M. D. De Vizia, F. Rohart, A. Castrillo, E. Fasci, L. Moretti, and L. Gianfrani, *Phys. Rev. A* **83**, 052506 (2011).
 - [6] M. Triki, C. Lemarchand, B. Darquié, P. L. T. Sow, V. Roncin, C. Chardonnet, and C. Daussy, *Phys. Rev. A* **85**, 062510 (2012).
 - [7] C. Lemarchand, S. Mejri, P. L. T. Sow, M. Triki, S. K. Tokunaga, S. Briaudeau, C. Chardonnet, B. Darquié, and C. Daussy, *Metrologia* **50**, 623 (2013).
 - [8] N. H. Ngo, H. Tran, and R. R. Gamache, *J. Chem. Phys.* **136**, 154310 (2012).
 - [9] H. Tran, N. H. Ngo, J.-M. Hartmann, R. R. Gamache, D. Mondelain, S. Kassi, A. Campargue, L. Gianfrani, A. Castrillo, E. Fasci, and F. Rohart, *J. Chem. Phys.* **138**, 034302 (2013).
 - [10] S. G. Rautian and I. I. Sobel'man, *Sov. Phys. Usp.* **9**, 701 (1967).
 - [11] R. Ciurylo and J. Szudy, *J. Quant. Spectrosc. Radiat. Transfer* **57**, 411 (1997).
 - [12] J. Keilson and J. E. Storer, *Q. J. Appl. Math.* **10**, 243 (1952).
 - [13] R. F. Snider, *Phys. Rev. A* **33**, 178 (1986).
 - [14] R. Ciurylo, A. Pine, and J. Szudy, *J. Quant. Spectrosc. Radiat. Transfer* **68**, 257 (2001).
 - [15] G. Nienhuis, *J. Quant. Spectrosc. Radiat. Transfer* **20**, 275 (1978).
 - [16] D. A. Shapiro, R. Ciurylo, R. Jaworski, and A. D. May, *Can. J. Phys.* **79**, 1209 (2001).
 - [17] P. Wcisło, A. Cygan, D. Lisak, and R. Ciurylo, *Phys. Rev. A* **88**, 012517 (2013).
 - [18] A. Pine, *J. Quant. Spectrosc. Radiat. Transfer* **62**, 397 (1999).
 - [19] M. Nelkin and A. Ghatak, *Phys. Rev.* **135**, A4 (1964).
 - [20] P. Berman, *J. Quant. Spectrosc. Radiat. Transfer* **12**, 1331 (1972).
 - [21] H. M. Pickett, *J. Chem. Phys.* **73**, 6090 (1980).
 - [22] J. Ward, J. Cooper, and E. W. Smith, *J. Quant. Spectrosc. Radiat. Transfer* **14**, 555 (1974).
 - [23] L. Fokin and A. Kalashnikov, *High Temp.* **46**, 614 (2008).
 - [24] D. Benner, C. P. Rinsland, V. Devi, M. A. H. Smith, and D. Atkins, *J. Quant. Spectrosc. Radiat. Transfer* **53**, 705 (1995).
 - [25] P. Amodio, L. Moretti, A. Castrillo, and L. Gianfrani, *J. Chem. Phys.* **140**, 044310 (2014).
 - [26] M. R. Moldover, R. M. Gavioso, J. B. Mehl, L. Pitre, M. de Podesta, and J. T. Zhang, *Metrologia* **51**, R1 (2014).
 - [27] B. H. McGuyer, R. Marsland, B. A. Olsen, and W. Happer, *Phys. Rev. Lett.* **108**, 183202 (2012).
 - [28] M. D. De Vizia, A. Castrillo, E. Fasci, L. Moretti, F. Rohart, and L. Gianfrani, *Phys. Rev. A* **85**, 062512 (2012).